Studying of Land Cover And Use Maps of South Asia Regions From 2001 To 2015 With AVHRR And MODIS Data

Shahzad Ali (ali88@hu.edu.pk)
Hazara University
Huang An Qi
Qingdao University
Malak Henchiri
Qingdao university
Zhang Sha
Qingdao University
Fahim Ullah Khan
Hazara University
Muhammad Sajid
Hazara University
Sajid Ali
Hazara University
Fengmei Yao
UCAS: University of the Chinese Academy of Sciences
Jiahua Zhang
UCAS: University of the Chinese Academy of Sciences

Research Article

Keywords: Random forest classification, Precision assessment, AVHRR GIMMS NDVI3g, land cover and land use, South Asia

Posted Date: September 17th, 2021

DOI: https://doi.org/10.21203/rs.3.rs-590999/v1

Abstract

In South Asia, annual land cover and land use (LCLU) is a severe issue in the field of earth science because it affects regional climate, global warming, and human activities. Therefore, it is vital essential to obtain correct information on the LCLU in the South Asia regions. LULC annual map covering the entire period is the primary dataset for climatological research. Although the LULC annual global map was produced from the MODIS dataset in 2001, this limited the perspective of the climatological analysis. This study used AVHRR GIMMS NDVI3g data from 2001 to 2015 to randomly forests classify and produced a time series of the annual LCLU map of the South Asia. The MODIS land cover products (MCD12Q1) are used as data from reference for trained classifiers. The results were verified using of the annual map of LCLU time series, and the space-time dynamics of the LCLU map were shown in the last 15 years, from 2001 to 2015. The overall precision of our 15-year land cover map simplifies 16 classes, which is 1.23% and 86.70% significantly maximum as compared to the precision of the MODIS data map. Findings of the past 15 years shows the changing detection that forest land, savanna, farmland, urban and established land, arid land, and cultivated land have increased; by contrast, woody prairie, open shrub-lands, permanent ice and snow, mixed forests, grasslands, evergreen broadleaf forests, permanent wetlands, and water bodies have been significantly reduced over South Asia regions.

Introduction

Changes in land cover and land use (LCLU) have always remained one of the main concerns in the development of sustainable agricultural management strategies that directly affect the hydrology, biodiversity and local climate (Linke et al., 2009). The LCLU information and its changes over time are very important for assessing the influence on the humans, atmosphere, and world systems (Meyer and Turner, 1992; Di Gregorio, 2005; Ali et al., 2019a). The South Asia is the most affected by land cover and land use change detection (IUCN, 2010; Ali et al., 2019b). The South Asia regions have facing water-related challenges, such as water shortage, low water use efficiency, and degradation of water quality. Furthermore, the South Asia region soon challenged a transition from pastoral-land to farm-land (Schulz et al., 2010; Ali et al., 2019a). The huge impact of land use, land use change and forestry on reducing livestock is another reason, which is related to the restoration of rain-fed farming (Olson et al., 20011). The land use and water resources have been greatly influenced by humans and ecosystems in South Asia have undergone some variations, such as the transformation of wet-lands to dry-lands and the melting of glaciers (Propastin and Muratova, 2008b). In addition, the South Asia regions is covered mostly by grasslands, grasslands savanna, open bushes and nearby bushes are involved in local and global carbon storage (Propastin and Muratova, 2008a). The climate change has been driver by deforestation, function of ecosystems and biodiversity (Tapia-Armijos et al., 2015). In the South Asia regions where natural assets are inadequate, which created an ecological problems in present and future, the forestry sector must improve forest ecosystems based on resources (Laurance et al., 2002).

For climate research, the dataset generated by MODIS (MCD12Q1) was used for LCLU (Lawrence and Chase 2007; Du et al., 2015). Only remote sensing data can provide accurate global LULC for monitoring drought and climate change (Muhammad et al., 2015). The global data set of NOAA-AVHRR images with high temporal frequency and high spatial resolution use to study the land change detection in the South Asia regions (Keith et al., 2014; Liu et al., 2018). In general, the dataset of MODIS is used in combination of dataset of AVHRR to study the land surface conditions on a large scale (James and Kalluri 1994; Jin and Zhang 2019). As described by Friedl et al. (2010) that the images of AVHRR have a continental and global scale old long history. He et al. (2017) reported that due to the accessibility of a higher spatial resolution, higher signal, and better remote-sensing data-sets such as MODIS sensors, the classification of AVHRR data sets has received less attention recently. The AVHRR data set contains the longest global image time series. It deals the probability of generating a time series of LCLU maps for long-term, which is an essential climatological research element. MODIS and AVHRR data are generally combined for land surface conditions and LCLU changing detection maps (Running et al., 1994; Ali et al., 2019a).

In Asia, the South Asia is one of the major important regions, providing a large number of services for economic growth and the world's population, whereas the South Asia contributes only 24% to the world's population with 3% world's land area (Bloom and Rosenberg, 2011; Fu et al., 2018). The total population increased from 473 million to 1.6 billion during 1950 to 2009, more than tripled, and is expected to grow by 41% by the end of 2050 (United Nations, 2009; Henchiri et al., 2019; Du et al., 2015). In the world the south Asia is one of the most ecologically diverse regions (Schneider et al., 2009; Fu et al., 2018; Huang et al., 2017). According to the (http:///://www.cepf. net/) the climatic regions of South Asia are distributed in the high-altitude areas in Afghanistan, in the south Indian Ocean, high mountains in the northwest, Himalayas in the north and the key points of biodiversity in the east of Bangladesh. Recent research has focused on generating a single AVHRR data map, which has not used for large area LCLU maps for time series. However, data-set of AVHRR is an important input for climatological research, and it is possible to generate time series for long-term LULC maps (Herold et al., 2008; Henchiri et al., 2019; Jin et al., 2019). In the present study, since the maximum spatial resolution data of MODIS can be obtained, AVHRR classification is considered to be less (Muhammad et al., 2015; Huang et al., 2017; Liu et al., 2018). The purpose of this study is to produce an annual LCLU map and an analysis of the changing detection between 2001 and 2015 over the South Asia regions. These maps are generated by using the random forest classification technique based on AVHRR GIMMS NDVI3g data set, and land cover product MCD12Q1 by using MODIS data. This study aims to generate a continuous time series covering the annual LCLU map of South Asia from 2001 to 2015, within the lasted 15 years. The spatial comparison of the study area is used to determine the magnitude of the change detection and the LCLU category is determined over the South Asia region.

Study Area And Data Sets

2.1. Study area

The study area includes 8 countries in South Asia, ranging from 114˚09′-122˚43′E, 34˚22′-38˚23′N. South Asia encompasses tropical and subtropical regions, including various climatic zones in the west and north. India and Afghanistan have temperate and arid regions in eastern regions of India and Pakistan. Figure 1 shows the mean sea level, geographic location, and elevation of land cover. From south to north, the elevation of South Asia varies greatly. India represents approximately 18% (1.3 billion) of the world population and is expected to overtake China in 2024 (United Nations, 2009). India represents

approximately 10% of world agricultural production (Alston and Pardey, 2014) and is expected to be greatly affected by global climate change (Goswami et al., 2006), Overgrowth and overuse of groundwater (Rodell et al. 2012).

2.2. Data Sets

The first data set used in this study is the first version of AVHRR GIMMS NDVI3g (2001–2015), which is a bimonthly compound generated from https://ecocast.arc.nasa.gov / data / pub / gimms / 3g.v1 /. According to the research of Pinzon and Tucker (2014), standardized GIMMS NDVI3g data can be used to solve some problems, such as the impact from the atmosphere, the loss of sensor calibration and orbital floatation. The spatial resolution of the data set is 1/12°. Then, we projected the NDVI3g dataset onto a geographic grid with WGS 198 ellipsoids, MODIS MCD12Q1 is the second dataset used in this study, namely WGS 198 4 ellipsoids, and re-sampled the initial MCD12Q1 from the MODIS sensor data set. At 1/12° pixels, it is equal to the AVHRR GIMMS NDVI3g dataset (Channan et al., 2014; Na et al., 2020). This data set is used as reference data for AVHRR classification to identify training areas and contains the LULC annual atlas from 2001 to 2015, corresponding to the classification system of the International Geosphere-Biosphere Project (IGBP).

2.3. Pre-processing of data

2.3.1. Classification

The study area includes large types of landforms, as well as ecological and climatic settings. Our goal is to select training data to classify it to capture geographic and temporal changes and detect changes in LCLU. We follow He et al., (2017) for the classification and evaluation of precision. Table 1 shows the LULC pixels unchanged in each area. To some extent, LCLU types were excluded from further analysis, reducing the original 17 classes to 16 LCLU classes. Forest randomization consists of a large number of classification trees, which vote on the results of each pixel (He et al., 2017). In addition to the classifier estimates the importance of each variable by summarizing the precision of the tree that does not use that variable (He et al., 2017).

Table 1 Number of pixels for each unchanged LULC type in the study area, with 25% used for training, and 75% for validation.

MODIS MCD12Q1 class	Number of pixels	Class for AVHRR classification
Evergreen Needleleaf Forests	128473	Evergreen Needleleaf Forests
Evergreen Broadleaf Forests	51004	Evergreen Broadleaf Forests
Deciduous Needleleaf Forests	0	Deciduous Needleleaf Forests
Deciduous Broadleaf Forests	81789	Deciduous Broadleaf Forests
Mixed Forests	114	Mixed Forests
Closed Shrublands	196012	Closed Shrublands
Open Shrublands	140998	Open Shrublands
Woody Savannas	160523	Woody Savannas
Savannas	544814	Savannas
Grasslands	18647	Grasslands
Permanent Wetlands	2041977	Permanent Wetlands
Croplands	43052	Croplands
Urban and Built-up Lands	56560	Urban and Built-up Lands
Cropland/Natural Vegetation Mosaics	19456	Cropland/Natural Vegetation Mo-saics
Permanent Snow and Ice	849519	Permanent Snow and Ice
Barren	27942	Barren
Water Bodies	7105	Water Bodies

2.3.2. Accuracy assessment and comparison

We have chosen several methods to calculate the reliability of the 15-year time series classified maps of the LULC map and represent such a complex dataset. This includes 75% of the validation data for comparison; the total duration is from 2001 to 2015, and the MCD12Q1 LULC mapping product was used in the classification of the training data. Tucker et al. (2005) showed that this evaluation can significantly introduce information on the successful replication of AVHRR NDVI. The usual model indicates that the sensor has the spectral advantages and radiation resolution of MODIS data.

2.3.3. Kappa statistics

Kappa statistics were also performed to determine the categorization precision of all the elements in the confusion matrix (Pontus and Millones, 2011). Further comparisons, there is a call to normalize the confusion matrix to unify the sum of each row and column (Warren, 2015).

The Kappa statistics calculation formula is as follows.

$$K = \frac{N\sum_{i=1}^{X} X_{ii} - \sum_{i=1}^{r}(X_{i+} \times X_{+i})}{N^2 - \sum_{i=1}^{r}(X_{i+} \times X_{+i})}$$

Where N = samples in the matrix, r = rows in the matrix, Xii is the number in the i-th row and the i-th column, X + i is the total number in the i-th row, and Xi + is the total number in the i-th column.

2.3.4. Land cover and use changing detection

Post-classification detection technology is used to detect changes in land use and coverage. Use pixel-based comparisons to generate pixel-by-pixel change information. To find-out the qualitative and quantitative change from 2001–2005, 2005–2010 and 2010–2015, a cross table was used to evaluate the classified image pairs.

Results And Discussion

3.1. Accuracy assessment and comparison

First, we evaluated the reliability of the classification of the AVHRR data. This is done by comparing the 75% validation data and LUDIS mapping associations of the MODIS during 2001, 2005, 2010, and 2015 products. These comparisons with MODIS data and 75% validation data are based on AVHRR classification have 16 categories presented in Table 1. After comparison, we report the results of more routine precision assessments. In the following sections, we summarize geographic and temporal trends from the 15-year time series after the precision assessment. In addition, we present the results of the precision assessment based on 9 LCLU visual interpretation classes. We describe the changes in the LCLU test after the precision assessment. We describe the changes in the LCLU test after the precision assessment. The focus of change detection analysis is the area of land distributed in the last 15 years.

3.2. LC LU classification with MODIS MCD12Q1 compared

The consistency value of the year used for classifier training is > 75% (Fig. 1). In training the classifier, we used several years to compare the entire MCD12Q1 chart. The results show that the classifier can infer different years from those used in training. Potentially, this can give information on the degree of success of AVHRR data-set in reproducing the general pattern recognized by MODIS having a sensor with excellent radiation and spectral resolution. To further study the consistency of each LCLU class among these two data sets, we provided producer and user constancy time series for each type of LCLU class from 2001 to 2015 (Fig. 2). The year used for training may be different from the annual temperature or precipitation. The consistency of various categories between these two LULC data sets will be further explored. For each category from 2001 to 2015, we show the consistency of the user's time series. The time series is determined as the consistency of the Category I pixels of the entire Category I pixels on the Classification Map, and the producer consistency is determined as Pixels Consistent of Class I pixels. All the pixels of the i-th category in the MODIS data (Fig. 2). Each year, the most consistent categories of producers and users are often open bush land, mixed forest, savanna, woody savanna, permanent wetland, grassland, arid and cultivated land. The categories with the least consistency between producers and users are bush land, land cultivated with natural vegetation, permanent ice and snow, bodies of water, urban and construction land. This may be due to the bigger size of the training sample and the better performance of the random forest classification as show in Table 1.

3.3. LULC classification with 75% internal comparison verification data

Identifying possible sources of error and evaluating the quality accuracy of the map is the most excellent approach to obtain such information. Foody, (2002) characterize the precision of the classification outcome derivative from the remote sensing data and the confusion matrix or the error matrix has been converted into a standardized remote sensing tool. The largest category in South Asia clearly shows that the accuracy of producers and users is often unlikely to be affected by cloud pollution. It is worth noting in Table 1 that open shrub-lands, mixed forests, savannas, croplands, permanent wetlands, woody savannas, permanent snow and ice and grasslands tend to cover largest number of training samples with high regional precision. Compared to the consistency value MCD12Q1, the consistency value of our classify map of LCLU is usually lower. Figure 2 summarizes the consistency of the producers and users of LULC that we divided for each class during the study period 2001–2015. Mixed forest, wooded savanna, open shrub-lands, grasslands, savanna, farmland, permanent wetlands, and barren lands are highly consistent, while closed shrub-lands, water bodies, urban and construction lands, permanent snow and ice and natural vegetation mosaics have less (Fig. 2). The Kappa coefficients in 2001, 2005, 2010 and 2015 were 86.5%, 85.8%, 85.5% and 84.2%, respectively.

3.4. Change detection analysis

For a more detailed analysis, we selected the changes in land cover in 2001–2005, 2005–2010 and 2010–2015 with a study interval of five years. Table 2 shows that the category of evergreen coniferous forest decreased by 6,249 km^2 during 2001–2005, then increased by 5,522 km^2 from 2005–2010 and decreased by 18,932 km^2 in the last five years of 2010–2015. The evergreen broadleaf forest category increased by 3,633 km^2 during 2001–2005, then increased again by 3,060 km^2 during 2005–2010, and decreased by 4,031 km^2 in the last five years of 2010–2015. The broadleaf deciduous forest category decreased by 1,716 km^2 during 2001–2005, then increased by 7084 km^2 during 2005–2010, and decreased by 26,821 km^2 in the last five years of 2010–2015. Between 2001 and 2005, the mixed forest category increased by 13,507 km^2, between 2005 and 2010 it increased by 8,644 km^2 and during the last five years of 2010–2015 it decreased by 37,976 km^2. During the period 2001–2005, the category of closed shrub land increased by 1,518 km^2, then decreased by 3,426 km^2 in 2005–2010, and increased by 5,543 km^2 in the last five years of 2010–2015. The open shrub-lands increase with 24642 Km^2 during the 2001–2005, and then decreased with 9455, and 2020 Km^2 during the 2005–2010, and 2010–2015. The grasslands increase with 45495 Km^2 during the 2001–2005, and then decreased with 14804, and 12794 Km^2 during the 2005–2010, and 2010–2015. During the 2005–2010, and 2010–2015 the croplands decreased with 16699 Km^2 during the 2001–2005, and then increased with 2862, and 119800 Km^2. During the 2010–2015 the permanent snow improved with 1646, and

14213 Km^2 during the 2001–2005 and 2005–2010, and then decreased with 81254 Km^2, respectively. From 2001 to 2015, the water bodies have decline by 9747, 4007 and 20868 km^2, respectively.

Table 2 Land cover/land use classes and change detection areas for each class in Km^2.

Map unit	Area 2001		Area 2005		Area 2010		Area 2015		change detection area km^2		
	km^2	%	km^2	%	km^2	%	km^2	%	2001-2005	2005-2010	2010-2015
Evergreen Needleleaf Forests	60058	1.18	53809	1.06	59331	1.17	40399	0.80	-6249	5522	-18932
Evergreen Broadleaf Forests	95840	1.89	99473	1.96	102533	2.02	98502	1.94	3633	3060	-4031
Deciduous Broadleaf Forests	179946	3.55	178230	3.51	185313	3.65	154342	3.04	-1716	7084	-26821
Mixed Forests	163092	3.22	176599	3.48	185243	3.65	147267	2.90	13507	8644	-37976
Closed Shrublands	6388	0.13	7902	0.16	4475	0.09	10018	0.20	1518	-3426	5543
Open Shrublands	370436	7.30	395078	7.79	385623	7.60	383596	7.56	24642	-9455	-2027
Woody Savannas	189413	3.73	187924	3.70	181168	3.57	167886	3.31	-1490	-6755	-13282
Savannas	293316	5.78	301190	5.94	292519	5.77	312510	6.16	7874	-8671	19990
Grasslands	688154	13.57	733649	14.46	718845	14.17	706052	13.92	45495	-14804	-12794
Permanent Wetlands	134840	2.66	127225	2.51	139493	2.75	135997	2.68	-7616	12269	-3496
Croplands	1504676	29.66	1487977	29.33	1490839	29.39	1610639	31.75	-16699	2862	119800
Urban and Built-up Lands	150653	2.97	147916	2.92	137622	2.71	147334	2.90	-2737	-10294	9712
Cropland/Natural Vegetation Mosaics	143226	2.82	131188	2.59	122675	2.42	137981	2.72	-12038	-8514	15307
Permanent Snow and Ice	83504	1.65	85150	1.68	99363	1.96	18110	0.36	1646	14213	-81254
Barren	912125	17.98	872104	17.19	884376	17.43	939655	18.52	-40021	12272	55279
Water Bodies	97156	1.92	87409	1.72	83402	1.64	62535	1.23	-9747	-4007	-20868
Total	5072822	100%	5072822	100%	5072822	100%	5072822	100%			

3.5. Annual Trends of LCLU over South Asia

During the 2001, 2005, 2010 and 2015, the annual LULC map of South Asia was generated by random forest classification method are showed in Fig. 3. It's worth noting that from 2001 to 2015, the pixels on the LULC map of South Asia did not change in South Asia derived from MCD12Q1 (Fig. 1). During the period of land use changing detection, and land change detection during 2001 to 2015, the map of South Asia was more or less similar. The results obtained indicate that the total area of the survey is 5.07 × 106 km^2 are presented in Table 2. The area is divided into 16 land cover categories. The cultivated land in South Asia decreased considerably between 2001 and 2005, and then increased between 2005 and 2015. The significantly reduction of grasslands and the popularization of current agronomic techniques have considerably increased cultivated land (Congalton & Green, 2009; Yuke, 2019; Na et al., 2020). In the past 15 years, cultivated land in South Asia has increased significantly, while grasslands, forest savannas, broadleaf deciduous forests, bodies of water, and permanent ice and snow have decreased. In contrast, closed bush land, savanna, natural vegetation per capita, barren land, urban land and urbanized in South Asia decreased from 2001 to 2005, but increased from 2005 to 2015 Trend (Table 2). Reddy et al. (2017) confirmed the recent decline of other species and the increase in cultivated land. In this study, the exchange between wetlands, barren areas, and woody shrub-land was significant exchange to crop-lands. In South Asia, compared to other categories, the overall increase and change pattern of cultivated land, our results are similar to those of Yin (2008). However, the basic reason for the basic analysis of various LULC courses in South Asia is beyond the capacity of this article.

Based on above mentioned analysis its confirm the clear spatial change patterns in water bodies, grass-lands, mixed forests, closed shrub-lands, evergreen needle-leaf forests, crop-lands, woody savannas, savannas, open shrub-lands, permanent snow and ice. In Fig. 4, 5, 6, and 7, are indicated the trends of overall 16 categories during the 15 years study period. The trend of the significance was use statistically package by using t-test. The generally trends for water bodies, mixed forests, deciduous broad-leaf forests, croplands, savannas, permanent snow and ice are a significant increase during 2001 to 2015 study duration. While, grass-lands, woody savannas, evergreen broad-leaf forests, closed shrub-lands, evergreen needle-leaf forests, urban lands, permanent wet-lands, open shrub-lands, barren and natural vegetation mosaics are overall showed decrease trend. This is consistent with He et al. (2017). The general crop-lands trend is an improving order from 2001 to 2015 durations. This may be due to change of Green to Grain (Jung et al., 2006; Yao et al., 2017). But, the uncertainty of these trends may be bigger due to larger standard errors of forest and crop-lands compared with grass-lands (Congalton & Green, 2009). Which may cause due to unusual climate conditions or other pressures and general policy changes (Pinheiro et al., 2014; Zhang et al., 2016; Yuke et al., 2019), our supposition is that these differences might be work of art such as sensor drift as the effect of chronological incompatible differences of GIMMS NDVI data. Earlier research work has indicated also these temporal inconsistencies of GIMMS NDVI value (Klein et al., 2012; Tian et al., 2015).

The confusion or error matrix has become a reliable technique to express the precision of the categorization results derived from remote sensing data (Ibrakhimov et al., 2007; Zhang et al., 2016). The error matrix provides three commonly used precision measures (Foody, 2002; Denisko and Hoffman, 2018), such as producer precision, user precision, and overall (Kotsiantis, 2007; Henchiri et al., 2019). To assess the correctness of the present categorization, we generated a confusion matrix based on the verification data set. Although the selected samples may be spatially related and the training process are not included. The results of the classification in 2001, 2005, 2010 and 2015 showed that the general precision was 87.65%, 86.95%, 86.67% and 85.55%. Tables 3, 4, 5 and 6show the confusion matrix for the classification of land cover, respectively.

Table 3 Confusion matrix of land covers classification 2001, expressed in percentages.

	Reference class														
	ENF	EBF	DBF	MF	CS	OS	WS	S	GL	PW	CL	UBL	NVM	PSI	B
Mapped class															
ENF	85.11	1.03	0.81				0.85	0.68	0.42		0.53				
EBF		93.81	2.44	0.61			2.54	1.37		1.49			1.75		
DBF		2.06	88.62	1.82			3.39	4.11	0.84			6.67	4.39		
MF	6.38	1.03	2.44	95.76			1.27	2.40	0.84	1.49	1.60		1.75		
CS					85.71										
OS						95.00			3.78	1.49		1.67		1.15	4.28
WS			1.63				89.41	3.08		4.48			3.51		
S	2.13	1.03	0.81		14.29		1.69	86.64	0.84	4.48	2.66	3.33	5.26		
GL	4.26		0.81	0.61		1.11			89.50		3.19	6.67	0.88		2.67
PW								0.34		85.07	1.60	8.33	2.63		
CL	2.13	1.03	0.81	1.21		0.56		1.03	0.84	1.49	89.89	10.00	4.39	1.15	1.60
UBL												63.33	0.88		
NVM			1.63				0.85				0.53		74.56		
PSI														81.61	2.14
B						3.33			2.94					16.09	89.30
WB								0.34							
PA	85.11	93.81	88.62	95.76	85.71	95.00	89.41	86.64	89.50	85.07	89.89	63.33	74.56	81.61	89.30
OA	87.65%														
KC	86.51%														

Table 4 Confusion matrix of land covers classification 2005, expressed in percentages.

	Reference class														
	ENF	EBF	DBF	MF	CS	OS	WS	S	GL	PW	CL	UBL	NVM	PSI	B
Mapped class															
ENF	87.23	3.09	0.81	1.21			1.69	0.68	0.42	1.49	0.53		2.63		
EBF		92.78	0.81	2.42			2.97	0.68		1.49					
DBF			91.06	1.21			2.97	1.37	0.84	1.49	1.60	3.33	1.75		
MF	8.51	1.03	2.44	92.12			4.24	4.11		2.99	0.53		2.63		
CS					85.71	0.56									
OS						96.11			2.94		0.53			2.30	7.49
WS			2.44				87.71	1.37	0.42	1.49			2.63		0.00
S	2.13	3.09		1.21	14.29			89.04		8.96	3.19	1.67	8.77		0.53
GL	2.13		1.63	0.61		0.56			90.76	1.49	3.72	5.00	2.63		1.60
PW				0.61				0.34		77.61	2.13	6.67	1.75		
CL			0.81				0.42	1.37	2.52	2.99	87.23	6.67	5.26	1.15	1.07
UBL								0.34				76.67	1.75		0.53
NVM				0.61				0.34			0.53		70.18		
PSI														74.71	1.60
B						2.78			1.68					21.84	87.17
WB								0.34	0.42						
PA	87.23	92.78	91.06	92.12	85.71	96.11	87.71	89.04	90.76	77.61	87.23	76.67	70.18	74.71	87.17
OA	86.95%														
KC	85.75%														

Table 5 Confusion matrix of land covers classification 2010, expressed in percentages.

	Reference class														
	ENF	EBF	DBF	MF	CS	OS	WS	S	GL	PW	CL	UBL	NVM	PSI	B
Mapped class															
ENF	85.11	2.06	2.44	1.82				1.37	0.42		0.53				
EBF		91.75	1.63	2.42			7.20	1.03	0.42		0.53		2.63		
DBF			87.80	3.64			3.81	2.40	2.10	1.49	2.66	5.00	3.51		
MF	6.38	2.06	2.44	90.30			3.81	2.74	0.42	5.97	0.53	1.67	6.14		
CS					85.71	0.56			0.42						
OS						98.33			2.10	1.49	0.53				2.67
WS			1.63	0.61			83.90	2.40			1.06		5.26		
S	2.13	2.06	1.63	0.61	14.29		0.85	87.67	1.26	2.99	2.13	3.33	3.51		
GL	4.26		1.63	0.61					88.66	1.49	4.26	3.33			2.14
PW		1.03					0.42			83.58	2.66	6.67	0.88		
CL	2.13					0.56		1.37	2.52	2.99	84.57	13.33	4.39		0.53
UBL								0.34				66.67	0.88		
NVM		1.03	0.81					0.34			0.53		72.81		
PSI														80.46	0.53
B						0.56			1.68					19.54	94.12
WB								0.34							
PA	85.11	91.75	87.80	90.30	85.71	98.33	83.90	87.67	88.66	83.58	84.57	66.67	72.81	80.46	94.12
OA	86.67%														
KC	85.45%														

Table 6 Confusion matrix of land covers classification 2015, expressed in percentages.

	Reference class														
	ENF	EBF	DBF	MF	CS	OS	WS	S	GL	PW	CL	UBL	NVM	PSI	B
Mapped class															
ENF	68.09	1.03					1.69	0.34			0.53		0.87		
EBF	2.13	93.81		1.82			2.54	1.37							
DBF	2.13		93.50	5.45			3.39	2.74	0.42	1.49		1.61	6.09		
MF	8.51	2.06	2.44	86.67			4.66	3.08	0.42		0.53	3.23	2.61		
CS					85.71				0.42						
OS						93.26			2.53		1.06	1.61			3.74
WS	2.13	1.03	1.63	2.42			84.75	1.03	0.00				3.48		
S	6.38	2.06	0.81	2.42	14.29		1.27	86.99	2.53	2.99	2.66	3.23	4.35		
GL	8.51		0.81	0.61		2.25			86.92	2.99	4.26	16.13	3.48	1.16	1.07
PW								1.03		83.58	1.60		2.61		0.53
CL	2.13						0.85	2.05	3.38	2.99	88.30	16.13	5.22		1.07
UBL								0.34			0.53	56.45			
NVM			0.81	0.61			0.85	0.68	0.42				71.30		
PSI														90.70	
B						3.93			2.53	5.97	0.53	1.61		8.14	93.05
WB						0.56		0.34	0.42						0.53
PA	68.09	93.81	93.50	86.67	85.71	93.26	84.75	86.99	86.92	83.58	88.30	56.45	71.30	90.70	93.05
OA	85.55%														
KC	84.20%														

Conclusion

The land covered and land use (LCLU) changing detection in South Asia have under major changes, including cultivated land, grasslands, mixed forests, urban and planted forests. The highest precision of producers and users in open shrubs, mixed forests, croplands, grasslands, permanent snow and badlands indicates that separating the categories from the larger reference data allows better random classification of forests. The overall 86.70% accuracy and 85.48% is the static kappa value. In addition to user accuracy for deciduous broadleaf forest, producer accuracy for the built-up and urban, water bodies and mosaic is also very small. However, due to the relatively small sample size, the uncertainty in this estimate is quite large. The categories with the highest levels of users and producers (> 75%) can be those of mixed forests, savannas and farmland. Tests of change carried out during 2001–2005, 2005–2010 and 2010–2015 showed that during 2001–2015, shrub-lands, barren, crop-lands, cropland/natural mosaics vegetation, savannas built-up and urban land are increase notably. In contrast, mixed forests, evergreen broadleaf forests, woody savannahs, evergreen coniferous forests, grasslands, permanent wetlands, open shrubs, permanent snow and water notably decrease. The verification and classification techniques used in this research work will be the basic data set for future climate studies, since the study will limit the accessibility of LCLU time series maps.

Declarations

Acknowledgements and Funding

This work was supported by the Key basic research project of Shandong natural science foundation of China (ZR2017ZB0422), the China Postdoctoral Science Foundation Project Funding (2018M642614), and “Taishan Scholar” project of Shandong Province.

Availability of data and materials

The availability of data and materials on the base of personal request.

Authors’ contributions

The manuscript was reviewed and approved for publication by all authors. FY and JZ conceived and designed the experiments. SA[1] and MH performed the experiments. SA[1], ZS,FUK, MS, SA[2] and MH analyzed the data. SA[1] and HAQ wrote the paper. SA[1], MH, ZS, FH, FY and JZ reviewed and revised the paper.

Compliance with ethical standards

Conflict of interest

The authors declare that they have no conflict of interest.

Ethical approval

The manuscript was reviewed and ethical approved for publication by all authors.

Consent to participate

The manuscript was reviewed and consents to participate by all authors.

Consent to publish

The manuscript was reviewed and consents to publish by all authors.

References

1. Ali S, Deming T, Zhen TX, Malak H, Kalisa W, Shi S, Jiahua Z (2019a) Characterization of drought monitoring events through MODIS and TRMM-based DSI and TVDI over South Asia during 2001–2017. Environmental Science and Pollution Research, doi.org/10.1007/s11356-019-06500-4
2. Ali S, Zhen TX, Henchiri M, Wilson K, Jiahua Z (2019b) Studying of drought phenomena and vegetation trends over South Asia from 1990 to 2015 by using AVHRR and NASA's MERRA data. Environmental Science Pollution Research. doi.org/10.1007/s11356-019-07221-4
3. Alston, Julian M, Pardey PG (2014) Agricultural r&d, food prices, poverty and malnutrition redux. staff papers
4. Andres L, Salas WA, Skole D (1994) Fourier analysis of multi-temporal AVHRR data applied to a land cover classification. Int J Remote Sens 15:1115–1121
5. Aronoff S (1985) The minimum accuracy value as an index of classification accuracy. Photogrammetric Engineering Remote Sensing 51:99–111
6. Baudron P, Alonso-Sarría F, García-Aróstegui JL, Cánovas-García F, Martínez-Vicente D, Moreno-Brotóns J (2013) Identifying the origin of groundwater samples in a multi-layer aquifer system with random Forest classification. J Hydrol 499:303–315
7. Bloom DE, Rosenberg L (2011) The Future of South Asia: Population Dynamics, Economic Prospects, and Regional Coherence. WDA-Forum, University of St. Gallen, http://www.cepf.net
8. Breiman L (2001) Random forests. Mach Learn 45:5–32
9. Channan S, Collins K, Emanuel W (2014) Global Mosaics of the Standard MODIS Land Cover Type Data. University of Maryland and the Pacific Northwest National Laboratory, College Park
10. Congalton RG, Green K (2009) Assessing the accuracy of remotely sensed data: Principles and practices. Lewis Publishers
11. Czaplewski RL (1992) Misclassification bias in areal estimates. Photo-grammetric Engineering Remote Sensing 58:189–192
12. Dahinden C (2011) An improved random forest approach with application to the performance prediction challenge datasets. Hands-on Pattern Recognition, Challenges in Machine Learning. 1, pp. 223–230
13. Dappen P (2003) Using Satellite Imagery to Estimate Irrigated Land: A Case Study in Scotts Bluff and Kearney Counties. Center of Advanced Land Management Information Techonologies. University of Nebraska-Lincoln, NE
14. Denisko D, Hoffman MM (2018) Classification and interaction in random forests. Proc. Natl. Acad. Sci. U. S. A. 115, 1690–1692
15. Dhiraj Goswami Kun-han, Tsai M, Kassab, & Takeo Kobayashi. 2006. At-speed testing with timing exceptions and constraints-case studies
16. Di Gregorio A (2005) Land cover classification system (LCCS), classification concepts and user manual, software version 2. Food and Agriculture Organization (FAO) of the United Nations, Rome
17. Du J, Shu J, Xinjie J, Jiaerheng A, Xiong S, He P, Liu W (2015) Analysis on spatio-temporal trends and drivers in vegetation growth during recent decades in Xinjing, China. Int J Appl Earth Obs Geoinf 38:216–228
18. El Saleous N (2005) An extended AVHRR 8-km NDVI dataset compatible with MODIS and SPOT vegetation NDVI data. Int J Remote Sens 26:4485–4498
19. Foody GM (2002) Status of land cover classification accuracy assessment. Remote Sens Environ 80:185e201
20. Friedl MA, Sulla-Menashe D, Tan B, Schneider A, Ramankutty N, Sibley A, Huang X (2010) MODIS collection 5 global land cover: algorithm refinements and characterization of new datasets. Remote Sens Environ 114:168–182
21. Fu Q, Zhou ZQ, Li TX, Liu D, Hou RJ, Cui S, Yan PR (2018) Spatiotemporal 10 characteristics of droughts and floods in northeastern China and their impacts on agriculture. Stoch. Environ. Res. Risk Assess. (10), 2913–2931
22. He Y, Lee E, Timothy AW (2017) A time series of annual land use and land cover maps of China from1982 to 2013 generated using AVHRR GIMMS NDVI3g data. Remote Sens Environ 199:201–217
23. Henchiri M, Ali S, Bouajila E, Wilson K, Sha Z, Yun B (2019) Monitoring land cover change detection with NOAA-AVHRR and MODIS remotely sensed data in the North and West of Africa from 1982 to 2015. Environmental Science Pollution Research. doi.org/10.1007/s11356-019-07216-1
24. Herold D, Mayaux P, Woodcock CE, Baccini A, Schmullius C (2008) Some challenges in global land cover mapping: an assessment of agreement and accuracy in existing 1 km datasets. Remote Sens Environ 112:2538e2556
25. Holben BN (1986) Characteristics of maximum-value composite images from temporal AVHRR data. Int J Remote Sens 7:1417–1434

26. Huang SZ, Ming B, Huang Q, Leng GY, Hou BB (2017) A Case Study on a Combination NDVI Forecasting Model Based on the Entropy Weight Method. Water Resour Manag 34:3667–3681
27. Ibrakhimov m, Khamzina A, Forkutsa I, Paluasheva G, Lamers JPA, Tischbein B et al (2007) Groundwater table and salinity: spatial and temporal distribution and influence on soil salinization in Khorezm region (Uzbekistan, Aral sea basin). Irrigat Drain Syst 21:219e236
28. IUCN, International Union for Conservation of Nature (2010) The Kazakh Steppe e Conserving the world's largest dry steppe region. http://www.iucn.org/about/ union/secretariat/offices/europe/resources/?5640/Kazakh-Action-Plan-for- Grasslands Accessed 10.02.12
29. James M, Kalluri SN (1994) The pathfinder AVHRR land data set: an improved coarse resolution data set for terrestrial monitoring. Int J Remote Sens 15:3347–3363
30. Jin J, Zhang NG (2019) Temporal and spatial evolution of drought index in Tibet. Soil water conservation research (05), 377–380 doi:10.13869/j.cnki.rswc.2019.05.054
31. Jung M, Henkel K, Herold M, Churkina G (2006) Exploiting synergies of global land cover products for carbon cycle modeling. Remote Sens Environ 101:534e553
32. Keith DJ, Schaeffer BA, Lunetta RS Jr, Rocha RWG, K., & Cobb DJ (2014) Remote sensing of selected water-quality indicators with the hyperspectral imager for the coastal ocean (hico) sensor. International journal of remote sensing 35(9–10):2927–2962
33. Klein I, Ursula G, Claudia K (2012) Regional land cover mapping and change detection in Central Asia using MODIS time-series. Appl Geogr 35:219e234
34. Kotsiantis SB (2007) Supervised machine learning: a review of classification techniques. Informatica 31:249e268
35. Laurance WF, Albernaz AK, Schroth G, Fearnside PM, Bergen S, Venticinque EM, Da Costa C (2002) Predictors of deforestation in the Brazilian Amazon. J Biogeogr 29:737–748
36. Lawrence PJ, Chase TN (2007) Representing a new MODIS consistent land surface in the Community Land Model (CLM 3.0). J Geophys Res Biogeosci 112:G01023
37. Liaw A, Wiener M, Breiman L, Cutler A (2009) Package "Randomforest". https://cran.rproject.org/web/packages/randomForest/randomForest.pdf Accessed 16. 04. 12
38. Linke J, McDermid GJ, Laskin DN, McLane AJ, Pape A, Cranston J, Hall-Beyer M, Franklin SE (2009) A disturbance-inventory framework for flexible and reliable landscape monitoring. Photogramm Eng Remote Sens 75:981–995
39. Liu H, Zhang M, Lin Z, Xu X (2018) Spatial heterogeneity of the relationship between vegetation dynamics and climate change and their driving forces at multiple time scales in southwest china. Agricultural and Forest Meteorology, s256–257, 10–21
40. Liu J, Heiskanen J, Aynekulu E, Maeda EE, Pellikka PK (2016) Land cover characterization inWest Sudanian Savannas using seasonal features from annual Landsat time series. Remote Sens 8:365
41. Lunetta RS, Knight JF, Ediriwickrema J, Lyon JG, Worthy LD (2006) Land-cover change detection using multi-temporal MODIS NDVI data. Remote Sens Environ 105:142–154
42. Mertens B, Lambin E (2000) Land-cover-change trajectories in southern Cameroon. Ann Assoc Am Geogr 90(3):467–494
43. Meyer WB, Turner II,BL (1992) Human population growth and global land use/land cover change. Annu Rev Ecol Syst 23:39e61
44. Muhammad S, Niu Z, Wang L, Aablikim A, Hao P, Wang C (2015) Crop classification based on time series MODIS EVI and ground observation for three adjoining years in Xinjiang. Spectrosc Spectr Anal 35:1345–1350
45. Na L, Haixia L, Tian xW, Yi L, Yi L, Xinguo C, Xiao tH (2020) Impact of climate change on cotton growth and yields in Xinjiang, China. Field Crops Research 247(2020) 107590
46. Olofsson P, Foody GM, Herold M, Stehman SV, Woodcock CE, Wulder MA (2014) Good practices for estimating area and assessing accuracy of land change. Remote Sens Environ 148:42–57
47. Olson DM, Dinerstein E, Wikramanayake ED, Burgess ND, Powell GN, Underwood MC (2001) Terrestrial eco-regions of the world: a new map of life on earth. Bioscience 51:933e938
48. Pinheiro J, Bates D, DebRoy S, Sarkar D (2014) Package "nlme". https://cran.r-project. org/web/packages/nlme/nlme.pdf Accessed 16. 12. 02
49. Pinzon JE, Tucker CJ (2014) A non-stationary 1981–2012 AVHRR NDVI3g time series. Remote Sens 6:6929–6960
50. Piper SE (1983) The evaluation of the spatial accuracy of computer classification. In: Proceedings of the 1983 Machine Processing of Remotely Sensed Data Symposium. West Lafayette: Purdue University, 303–310
51. Pontius RG, Millones M (2011) Death to Kappa: birth of quantity disagreement and allocation disagreement for accuracy assessment. Int J Remote Sens 32:4407–4429
52. Propastin PA, Kappas M, Muratova NR (2008a) Inter-annual changes in vegetation activities and their relationship to temperature and precipitation in Central Asia from 1982 to 2003. Journal of Environmental Informatics 12(2):75e87
53. Propastin PA, Kappas M, Muratova NR (2008b) A remote sensing based monitoring system for discrimination between climate and human-induced vegetation change in Central Asia. Management of Environmental Quality: An International Journal 19(5):579e596
54. Reddy CS, Pasha SV, Satish KV, Saranya KRL, Jha CS, Krishna Murthy YVN (2017) Quantifying nationwide land cover and historical changes in forests of Nepal (1930–2014): implications on forest fragmentation. Biodivers Conserv. http://dx. doi.org/10.1007/s10531-017-1423-8
55. Rodell M, Chen J, Kato H, Nigro FJ, Al E (2012) Grace and water loss from indo-ganga basin. Journal of the Geological Society of India
56. Rodriguez-Galiano VF, Ghimire B, Rogan J, Chica-Olmo M, Rigol-Sanchez JP (2012) An assessment of the effectiveness of a random forest classifier for land-cover classification. ISPRS J Photogramm Remote Sens 67:93–104

57. Rosenfield GH, Fitzpatrick-Lins K (1986) A coefficient of agreement as a measure of thematic classification accuracy. Photo-grammetric Engineering Remote Sensing 52:223–227
58. Rouse JW Jr, Haas R, Schell J, Deering D (1974) Monitoring Vegetation Systems in the Great Plains with ERTS. Proceedings of the Thrid ERTS Symposium, NASA, Washington, DC, USA, pp. 309–317
59. Running SW, Loveland TR, Pierce LL (1994) A vegetation classification logic based on remote sensing for use in global biogeochemical models. Ambio 23:77–81
60. Sabins J, Lulla K (2007) Remote Sensing: Principles and Interpretation. 3rd edition. Waveland, Illinois
61. Schneider A, Friedl MA, Potere D (2009) A new map of global urban extent from MODIS satellite data. Environ Res Lett 4:044003
62. Schulz JJ, Cayuela L, Echeverria C, Salas J, Benayas JMR (2010) Monitoring land cover change of the dry-land forest landscape of Central Chile (1975–2008). Appl Geogr 30(3):436–447
63. Tapia-Armijos MF, Homeier J, Espinosa CI, Leuschner C, de la Cruz M (2015) Deforestation and forest fragmentation in South Ecuador since the 1970s – losing a hotspot of biodiversity. PLoS One 10 (9), e0133701. http://dx.doi.org/10.1371/ journal.pone.0133701
64. TEl Saleous N (2005) An extended AVHRR 8-km NDVI dataset compatible with MODIS and SPOT vegetation NDVI data. Int J Remote Sens 26:4485–4498
65. Tian F, Fensholt R, Verbesselt J, Grogan K, Horion S, Wang Y (2015) Evaluating temporal consistency of long-term global NDVI datasets for trend analysis. Remote Sens Environ 163:326–340
66. Townshend J, Justice C, Li W, Gurney C, McManus J (1991) Global land cover classification by remote sensing: present capabilities and future possibilities. Remote Sens Environ 35:243–255
67. Tucker CJ, Pinzon JE, Brown ME, Slayback DA, Pak EW, Mahoney R, Vermote, E.F.
68. United, Nations (2009) World population prospects: The 2008 revision population database. http://esa.un.org/wup2009/unup/index.asp, Accessed date: 3 October 2015
69. Warrens MJ (2015) Properties of the quantity disagreement and the allocation disagreement. Int J Remote Sens 36:1439–1446
70. Wulder MA, White JC, Loveland TR, Woodcock CE, Belward AS, Cohen WB, Fosnight G, Shaw J, Masek JG, Roy DP (2016) The global Land-sat archive: status, consolidation, and direction. Remote Sens. Environ
71. Yao TD, Chen FH, Cui P et al (2017) From Tibetan Plateau to Third Pole and Pan-Third Pole. Bulletin of Chinese Academy of Sciences 32:924–931
72. Yin X (2008) Analysis on the change of land use by remote sensing technology in Manas county. J Shihezi Univ (Nat Sci) 26:402–406
73. Yuan F, Sawaya KE, Loeffelholz BC, Bauer ME (2005) Land cover classification and change analysis of the Twin Cities (Minnesota) Metropolitan area by multi-temporal Land-sat remote sensing. Remote Sens Environ 98:317–328
74. Yuke Z (2019) Characterizing the spatio-temporal dynamics and variability in climate extremes over the Tibetan plateau during 1960–2012. J Resour Ecol 10(4):397. https://doi.org/10.5814/j.issn.1674-764x.2019.04.007
75. Zhang J, Mu Q, Huang J (2016) Assessing the remotely sensed drought severity index for agricultural drought monitoring and impact analysis in North China. Ecol Indic 63:296–309

Figures

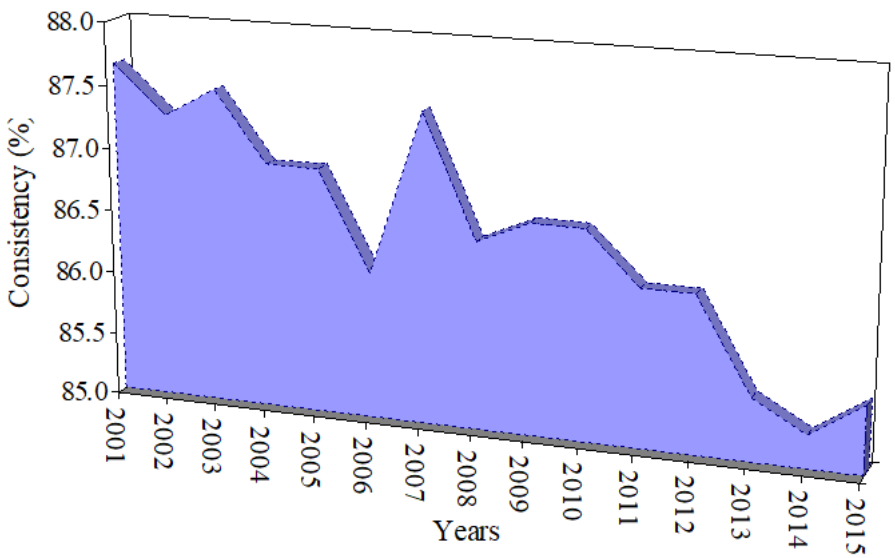

Figure 1

Consistency between classified LULC maps and MODIS MCD12Q1 from 2001 to 2015.

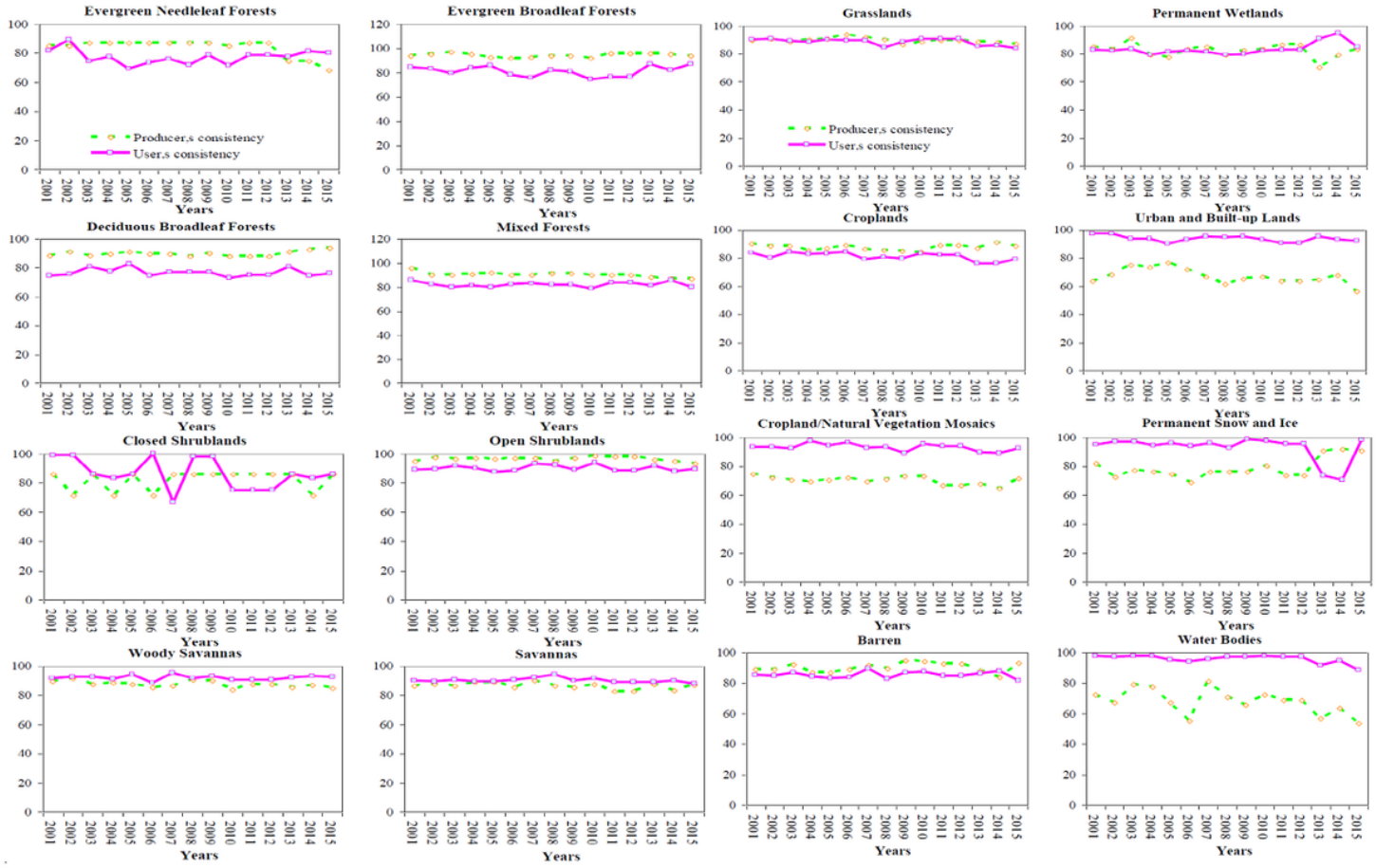

Figure 2

User's and producer's consistencies for each class between classified LULC maps and MODIS MCD12Q1 from 2001 to 2015.

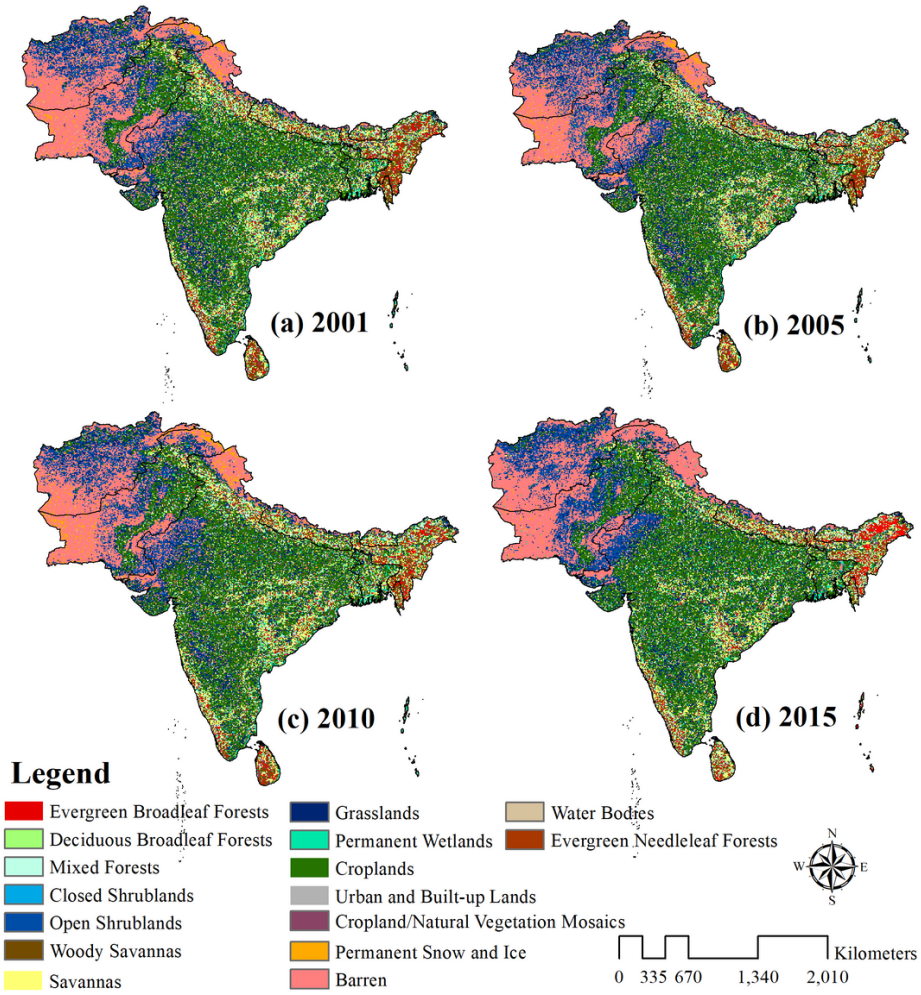

Figure 3

Annual LULC maps of South Asia, produced by random forest classification. (a) 2001, (b) 2005, (c) 2010, and (d) 2015.

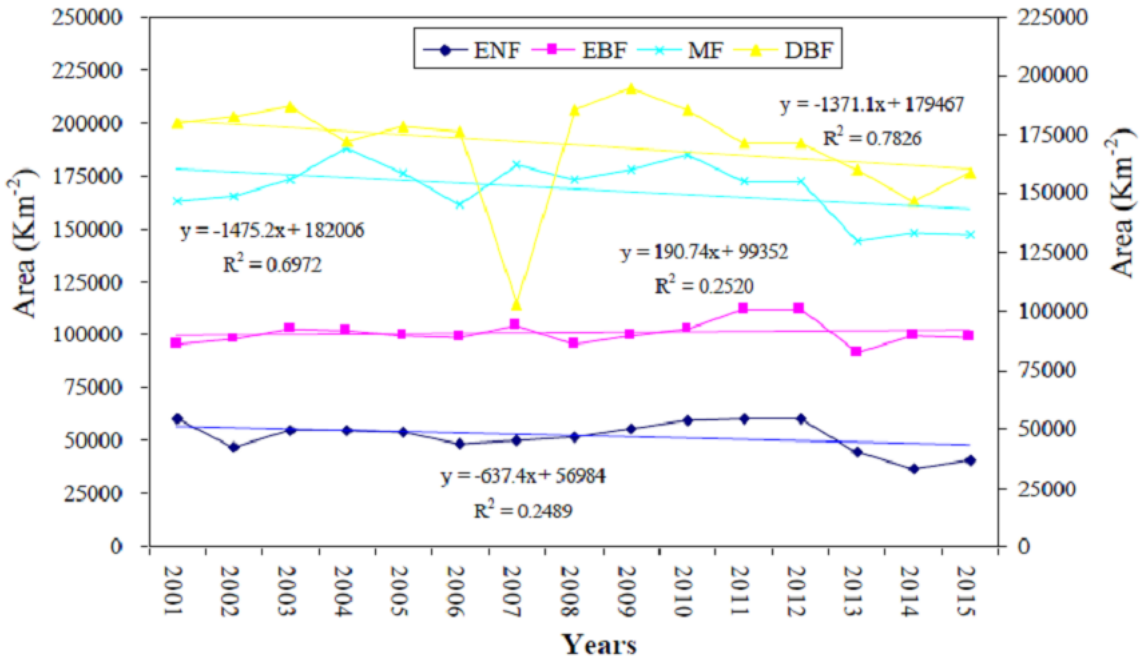

Figure 4

Temporal changes in area of evergreen needleleaf forests (ENF), evergreen broadleaf forests (EBF), mixed forests (MF) and deciduous broadleaf forests (DBF) classes from 2001 to 2015. Dotted lines represent overall trend.

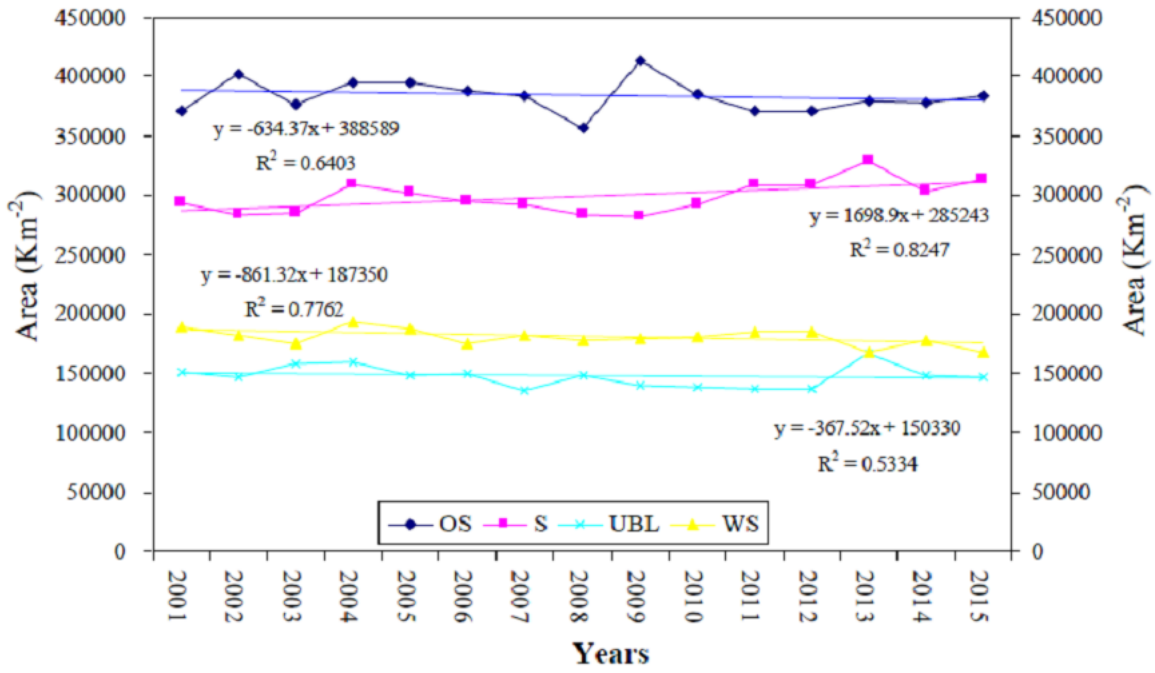

Figure 5

Temporal changes in area of open shrublands (OS), savannas (S), urban and built-up lands (UBL) and woody savannas (WS) classes from 2001 to 2015. Dotted lines represent overall trend.

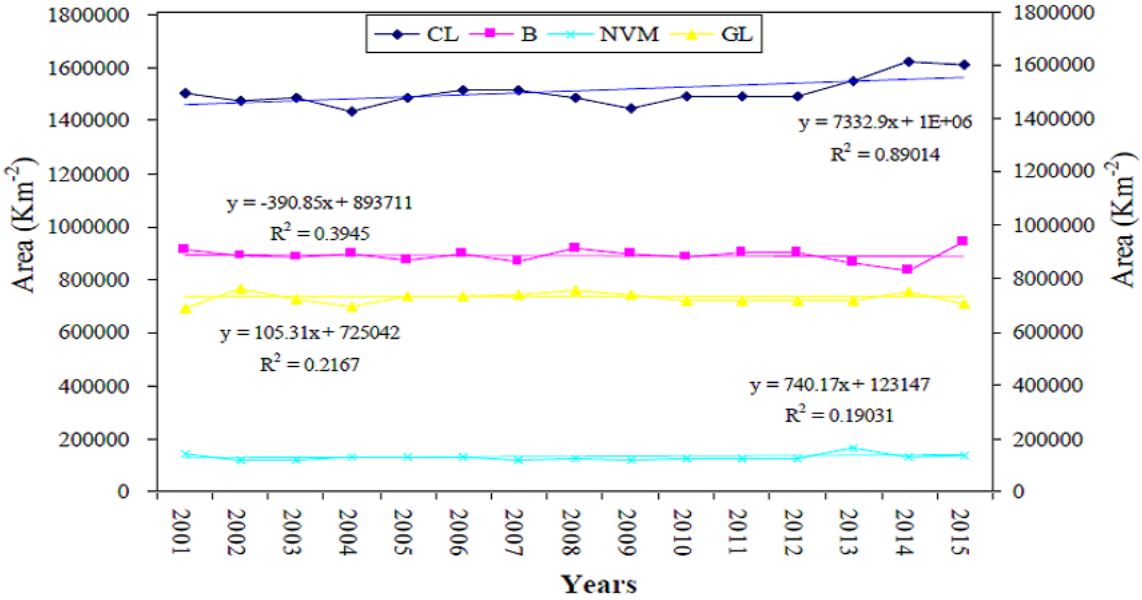

Figure 6

Temporal changes in area of croplands (CL), barren (B), cropland/natural vegetation mosaics (NVM) and grasslands (GL) classes from 2001 to 2015. Dotted lines represent overall trend.

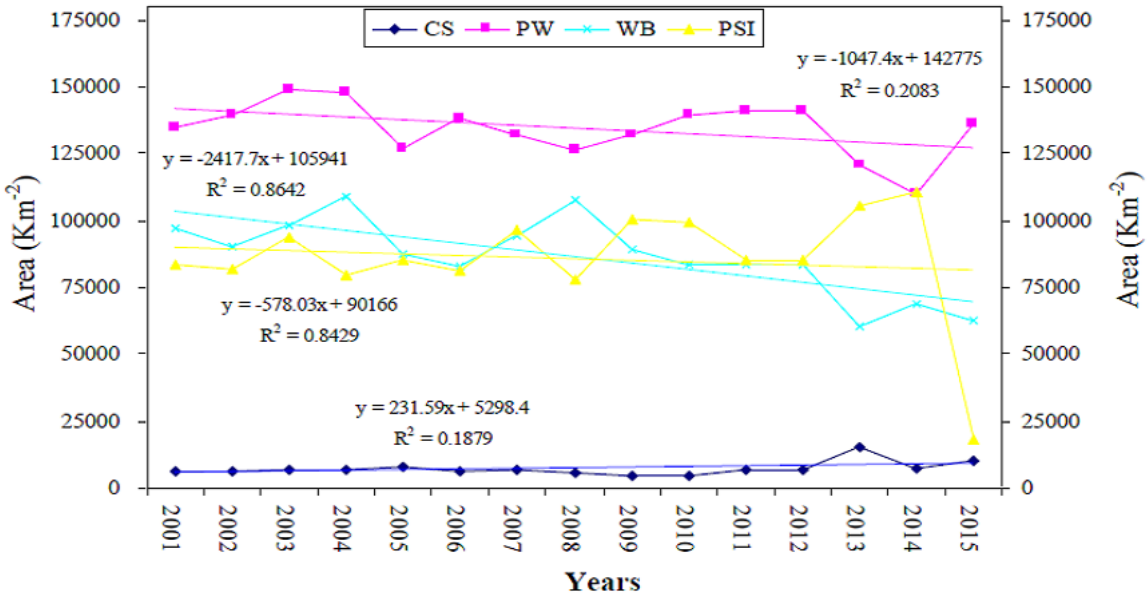

Figure 7

Temporal changes in area of closed shrublands (CS), permanent wetlands (PW), water bodies (WB) and permanent snow and ice (PSI) classes from 2001 to 2015. Dotted lines represent overall trend.